Available online at www.sciencedirect.com
SCIENCE DIRECT®
Journal of Organometallic Chemistry 690 (2005) 2044–2051
Journal of Organometallic Chemistry
www.elsevier.com/locate/jorganchem

A dihydrogen bond between a bridging hydride and the NH proton of a coordinated dimethylamine: solid state, solution and theoretical characterization

Monica Panigati [a,*], Pierluigi Mercandelli [b,*], Giuseppe D'Alfonso [a], Tiziana Beringhelli [a], Angelo Sironi [b]

[a] *Dipartimento di Chimica Inorganica, Metallorganica e Analitica, via Venezian 21, I-20133, Milano, Italy*
[b] *Dipartimento di Chimica Strutturale e Stereochimica Inorganica, via Venezian 21, I-20133, Milano, Italy*

Received 6 December 2004; accepted 7 December 2004
Available online 12 January 2005

Abstract

The addition of one equivalent of dimethylamine (DMA) to the 44 valence-electron triangular cluster anion $[Re_3(\mu_3\text{-}H)(\mu\text{-}H)_3(CO)_9]^-$ (**1**) affords the novel unsaturated derivative $[Re_3(\mu\text{-}H)_4(CO)_9(DMA)]^-$ (**2**, 46 valence electrons) which contains a dimethylamine molecule terminally coordinated to a cluster vertex. Theoretical calculations (DFT) reveal that in the more stable conformation the dimethylamine NH proton is directed towards the hydride bridging the opposite cluster edge in *syn* position, the close proximity of the ligands bound to the cluster surface allowing the formation of an unconventional N–H ⋯ (μ-H)Re_2 hydrogen bond. The presence of this conformation in the solid state has been proven by an X-ray structural analysis of crystalline $[PPh_4]$**2**. Spectroscopic evidences (IR and NMR) indicate that the dihydrogen bond is maintained also in solution and, by the evaluation of the proton spin-lattice relaxation rates at variable temperature, a good estimate of the H ⋯ H distance in solution has been determined.

Keywords: Cluster compounds; Density functional calculations; Hydride ligands; Hydrogen bonds; NMR spectroscopy; X-ray diffraction

1. Introduction

Since it was first reported [1], the occurrence of weak interactions between metal hydrides and hydrogen atoms bonded to electronegative main group atoms (N or O) has been the object of a great deal of research [2]. The term "dihydrogen bond" (DHB) was coined to distinguish this "unconventional" interaction from the classical X–H ⋯ Y hydrogen bonds (X and Y being highly electronegative main group atoms).

Only a few examples of DHB have so far been reported in cluster chemistry [3], and the proton acceptor has usually been found to be a terminally coordinated hydride. We have recently reported the first example of a DHB involving a bridging hydride in the triangular rhenium cluster anion $[Re_3(\mu\text{-}H)_4(CO)_9(HPz)]^-$, containing a pyrazole ligand terminally coordinated to a cluster vertex [4].

Here we present a second example of a N–H ⋯ (μ-H)Re_2 dihydrogen bond in a triangular rhenium cluster, involving a bridging hydride as a proton acceptor and the NH proton of a coordinated amine. The character-

* Corresponding authors. Tel.: +390250314447; fax: +390250314454 (P. Mercandelli).
E-mail addresses: monica.panigati@unimi.it (M. Panigati), pierluigi.mercandelli@unimi.it (P. Mercandelli).

0022-328X/$ - see front matter © 2004 Elsevier B.V. All rights reserved.
doi:10.1016/j.jorganchem.2004.12.003

ization of this interaction has been supported both by experimental evidence (IR, NMR and X-ray analysis) and theoretical computations (DFT).

2. Results and discussion

It has already been shown that the addition of two-electron donor molecules L to the "super-unsaturated" triangular cluster anion $[Re_3(\mu_3\text{-}H)(\mu\text{-}H)_3(CO)_9]^-$ (**1**, 44 valence electrons) [5] easily and selectively affords unsaturated $[Re_3(\mu\text{-}H)_4(CO)_9(L)]^-$ adducts (46 valence electrons), in which the ligand L occupies an axial position on the vertex of the cluster opposite to the Re-$(\mu\text{-}H)_2$Re basal interaction (see Scheme 1). On using dimethylamine $NHMe_2$ (DMA) as ligand L we have now quantitatively obtained the novel cluster anion $[Re_3(\mu\text{-}H)_4(CO)_9(DMA)]^-$ (**2**).

The ^{1}H NMR spectrum ($CDCl_3$, 298 K) shows three hydridic resonances at $\delta - 7.97$, -9.34 and -9.69 ppm, in 1:1:2 ratio, in agreement with the idealized C_s symmetry of anion **2**.

The rotational conformer of **2** depicted in Scheme 1, in which the NH proton points towards the hydride bridging the opposite cluster edge, has been found to be present in crystalline $[PPh_4]$ **2** by an X-ray structural analysis. DFT computations at the B3LYP/DZP level of theory also indicate that the more stable rotamer for anion **2** is that in which a hydrogen bond is formed. Spectroscopic investigations (IR and NMR) confirmed that this conformation is also the preferred one in solution, at least in solvents not able to act as proton acceptors.

2.1. Solid-state characterization of the anion $[Re_3(\mu\text{-}H)_4(CO)_9(DMA)]^-$ (2)

The molecular structure of anion **2**, as determined in a crystal of its $[PPh_4]^+$ salt, is depicted in Fig. 1 with a partial labelling scheme. A selection of bond parameters is reported in Table 1.

Anion **2** possesses an overall idealised C_s symmetry and contains an isosceles triangular metal core bearing nine terminal carbonyls, three to each rhenium atom, a dimethylamino ligand and four edge-bridging hydrido ligands. When considering the bonding interaction around the rhenium atoms, if the direct metal–metal interactions are neglected each metal attains a distorted octahedral coordination.

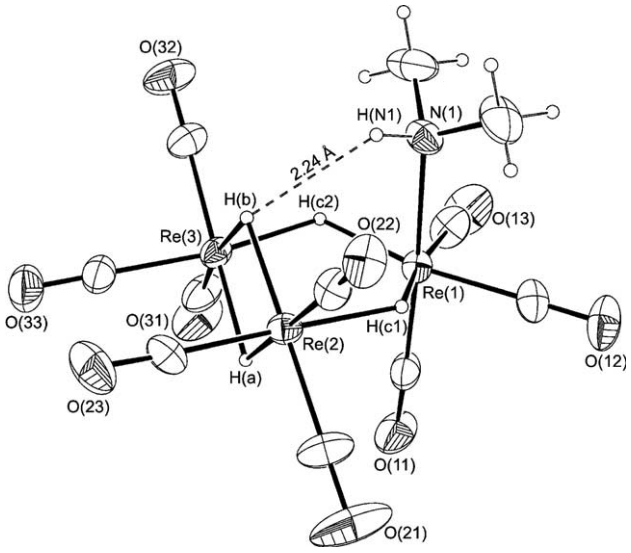

Fig. 1. ORTEP drawing of the $[Re_3(\mu\text{-}H)_4(CO)_9(DMA)]^-$ anion (**2**) with partial labelling scheme. Thermal ellipsoids are drawn at the 30% probability level. Hydrogen atoms were given arbitrary radii.

Cluster **2** shows two long Re–Re distances (mean value 3.182 Å) and one shorter interaction (2.799 Å) corresponding to a formal Re$(\mu\text{-}H)_2$Re formal double bond; a similar pattern has been observed in the related unsaturated clusters $[Re_3(\mu\text{-}H)_4(CO)_9L]^-$ (L = carbonyl, pyridine, triphenylphosphine, or pyrazole) [4,6].

As shown in Fig. 1, the H(N1) proton of the dimethylamino ligand bound to Re(1) forms a hydrogen bond with the hydride H(b), bridging the opposite cluster edge Re(2)–Re(3). The distance between H(N1) and H(b) is 2.239 Å; this distance has been computed using idealised positions for both the hydrogen atoms [7], even if they were found in a difference Fourier map, in order to avoid the systematic errors associated with X-ray diffraction determined hydrogen atom positions. The adoption of this conformation by anion **2** could be attributed to an attempt of avoid unfavourable steric interactions between the DMA methyl groups and the diagonal carbonyl ligands bound to the Re$(\mu\text{-}H)_2$Re moiety. However, the presence of a manifest attractive interaction can be inferred by the significant tilting of the dimethylamino ligand towards the bridging hydride

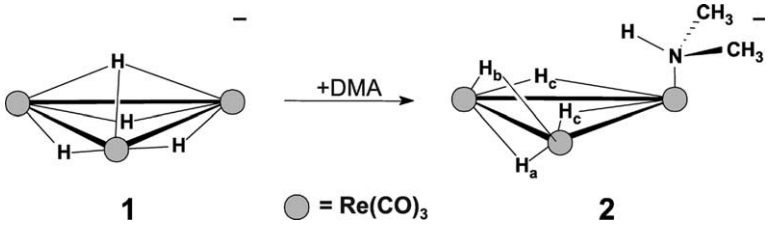

Scheme 1.

Table 1
Selected bond distances (Å) and angles (°) for the trinuclear complex **2**

Re(1)–Re(2)	3.1844(8)	Re(3)–C(31)	1.914(13)
Re(1)–Re(3)	3.1786(8)	Re(3)–C(32)	1.932(13)
Re(2)–Re(3)	2.7989(8)	Re(3)–C(33)	1.897(13)
Re(1)–N(1)	2.246(8)	N(1)–C(1)	1.456(16)
Re(1)–C(11)	1.889(12)	N(1)–C(2)	1.472(17)
Re(1)–C(12)	1.915(12)		
Re(1)–C(13)	1.924(13)		
Re(2)–C(21)	1.898(12)		
Re(2)–C(22)	1.914(11)		
Re(2)–C(23)	1.910(12)		
Re(2)–Re(1)–Re(3)	52.190(17)	Re(3)–Re(2)–C(21)	132.2(4)
Re(1)–Re(2)–Re(3)	63.799(15)	Re(3)–Re(2)–C(22)	137.4(3)
Re(1)–Re(3)–Re(2)	64.011(18)	Re(3)–Re(2)–C(23)	94.6(4)
Re(2)–Re(1)–N(1)	86.5(2)	C(21)–Re(2)–C(22)	89.9(5)
Re(2)–Re(1)–C(11)	90.3(4)	C(21)–Re(2)–C(23)	91.3(6)
Re(2)–Re(1)–C(12)	109.0(4)	C(22)–Re(2)–C(23)	89.9(5)
Re(2)–Re(1)–C(13)	158.7(4)	Re(1)–Re(3)–C(31)	98.9(4)
Re(3)–Re(1)–N(1)	88.5(2)	Re(1)–Re(3)–C(32)	108.7(4)
Re(3)–Re(1)–C(11)	88.5(3)	Re(1)–Re(3)–C(33)	159.2(4)
Re(3)–Re(1)–C(12)	160.7(4)	Re(2)–Re(3)–C(31)	133.3(4)
Re(3)–Re(1)–C(13)	106.7(4)	Re(2)–Re(3)–C(32)	134.2(4)
N(1)–Re(1)–C(11)	176.6(5)	Re(2)–Re(3)–C(33)	96.2(4)
N(1)–Re(1)–C(12)	95.3(4)	C(31)–Re(3)–C(32)	91.9(5)
N(1)–Re(1)–C(13)	96.3(5)	C(31)–Re(3)–C(33)	90.2(6)
C(11)–Re(1)–C(12)	87.0(5)	C(32)–Re(3)–C(33)	89.5(6)
C(11)–Re(1)–C(13)	86.2(6)	Re(1)–N(1)–C(1)	116.4(8)
C(12)–Re(1)–C(13)	91.7(5)	Re(1)–N(1)–C(2)	115.0(8)
Re(1)–Re(2)–C(21)	102.0(5)	C(1)–N(1)–C(2)	110.6(12)
Re(1)–Re(2)–C(22)	107.0(3)		
Re(1)–Re(2)–C(23)	158.4(4)		

(the angle between the Re(1)–N(1) vector and the Re_3 plane being 86.5(2)°).

Crystalline $[PPh_4]$ **2** presents additional interesting structural features. A short inter-molecular N–H ⋯ O hydrogen bonding interaction is observed between the hydrogen atom of the dimethylamino ligand and a carbonyl ligand of a symmetry-related anion, resulting in the formation of a dimer linked by two bifurcated hydrogen bonds (see Fig. 2). The structural parameters of this interaction are listed in Table 2.

The observed NH ⋯ H distance is somehow affected by the presence of this additional inter-molecular inter-

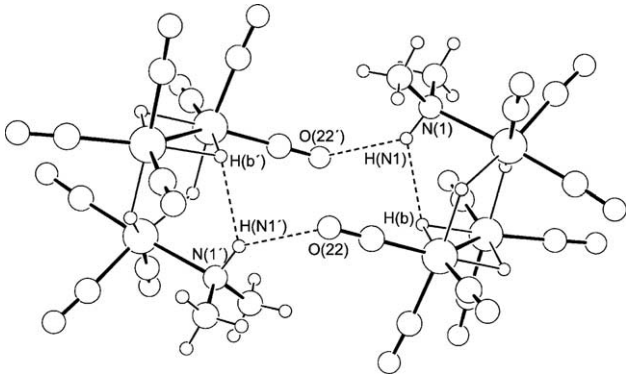

Fig. 2. Hydrogen bonding interactions in the crystal structure of $[PPh_4][Re_3(\mu\text{-}H)_4(CO)_9(DMA)]$.

Table 2
Relevant hydrogen bond parameters (Å and °) for $[PPh_4]$**2**[a]

N(1)–H(N1)	1.025
H(N1) ⋯ H(B)	2.239
H(N1) ⋯ O(22′)	2.332
N(1) ⋯ H(B)	3.032
N(1) ⋯ O(22′)	3.197(12)
N(1)–H(N1) ⋯ H(B)	133.0
N(1)–H(N1) ⋯ O(22′)	141.3
H(B)–H(N1) ⋯ O(22′)	85.5

[a] Primes refer to symmetry-related atoms ($-x$, $-y$, $1-z$).

action and should not be directly compared to the one measured in solution by NMR or to the one computed in vacuo (see below).

2.2. Theoretical characterization of the anion $[Re_3(\mu\text{-}H)_4(CO)_9(DMA)]^-$ (2)

The possible existence of different rotamers of anion **2** has been investigated by means of a DFT computational study. Computations have been done at the B3LYP/DZP level of theory (see Section 4 for details). The rotation of the dimethylamino ligand around the Re–N bond has been studied by driving the (improper) torsion angle ω H(b) ⋯ Re(1)–N(1)–H(N1).

Two rotamers can be identified, one corresponding to the dihydrogen bonded species found in the solid state (rotamer A, $\omega = 0$) and the other corresponding to a 180 rotation of the DMA ligand (rotamer B, see Fig. 3). Both conformations are found to be effective minima at the level of theory employed, although rotamer B lies on a very flat region of the potential energy surface.

A direct evaluation of the strength of an intra-molecular hydrogen bond is hampered by the impossibility of separating the two interacting fragments. A widely employed strategy to circumvent this problem consists in comparing the stability of two different conformations of the molecule in which the hydrogen bond is alternatively present and absent. The energy difference between the two rotamers A and B amounts to 5 kcal mol^{-1}. This value can only be taken as an upper limit for the strength of the dihydrogen bond, since rotamer A is stabilized with respect to B not only by the presence of this interaction but also by steric factors. Indeed, the presence of unfavourable steric interactions between the DMA methyl groups and the diagonal carbonyl ligands in rotamer B is clearly proven by the significant tilting of the coordination octahedra at the rhenium atoms and by the sizeable lengthening of the Re–N bond distance (2.341 Å) with respect to rotamer A (2.308 Å). However, the computed energy difference is in agreement with the observation of only rotamer A in dichloromethane solution, while in solvents able to act as effective hydrogen bond acceptors the possible presence of a significant amount of rotamer B can be anticipated (see below).

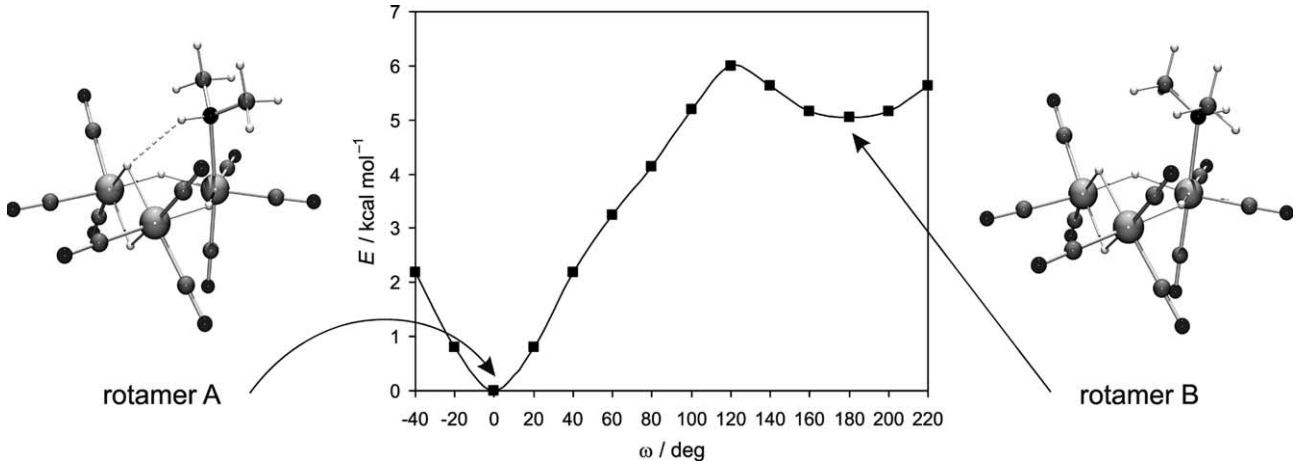

Fig. 3. B3LYP/DZP energy profile along the rotation of the dimethylamino ligand around the Re–N bond for anion **2**. The computed structures corresponding to the two minima, namely rotamer A and B, are also depicted.

The presence of a dihydrogen bond in rotamer A is further supported by some computed geometric and vibrational data. In particular, the N–H distance computed for rotamer A (1.021 Å) is stretched with respect to those computed for free DMA (1.016 Å) and for the non hydrogen bonded DMA moiety in rotamer B (1.017 Å). Moreover, as in the solid state structure, in rotamer A the Re–N vector is clearly bent towards the basal Re–Re edge, in agreement with the presence of an attractive interaction between NH and H_b. The ν(N–H) harmonic stretching frequency computed for rotamer A (3465 cm^{-1}) shows a significant shift to lower wavenumbers with respect to the ones computed for rotamer B (3515 cm^{-1}) and for the free DMA molecule (3526 cm^{-1}). The computed IR intensities $(\partial\mu/\partial q)^2$ are very sensitive to the local charge on the NH proton: the value found for rotamer A (57.0 a.u.) is indeed much larger than the ones found for rotamer B (8.3 a.u.) or free DMA (0.8 a.u.). In order to make a comparison with a classical hydrogen bond, the geometry of the dimethylamine dimer in its more stable C_s conformation has been optimised and a frequency computation has been carried out. The computed values [d(N–H) = 1.022 Å, ν(N–H) = 3428 cm^{-1}, $(\partial\mu/\partial q)^2$ = 225.8 a.u.] indicates that the dihydrogen bond present in anion **2** is weak compared to a classical N–H ⋯ N hydrogen bond.

In rotamer A, we compute an NH ⋯ H distance of 2.134 Å, in fair agreement with the experimental values measured both in the solid state and in solution. In order to compare the computed value to the better estimate in solution (2.24 Å, from the evaluation of T_1 at variable temperature, see below) the effect of the libration of the DMA ligand must be taken into account. The normal mode associated with the rotation around the Re–N bond (29 cm^{-1}) makes the major contribution to the lengthening of the H ⋯ H interaction. Employing standard Boltzmann statistics [8], we compute at 193 K an NH ⋯ H distance of 2.228 Å, in good agreement with the measured value.

2.3. Solution characterization of the dimethylamine conformation in anion 2

A 2D NOESY experiment, performed at 273 K in CD_2Cl_2, indicates the close proximity of the N–H proton to the bridging hydride H_b. First of all, the 2D map (Fig. 4) allows the identification of the H_b resonance as that of integrated intensity 1 which shows nOe cross-peaks with both the NH proton and the methyl groups of DMA. The same correlations are exhibited also by the hydridic signal of integrated intensity 2, due to the hydrides H_c bridging the lateral edges.

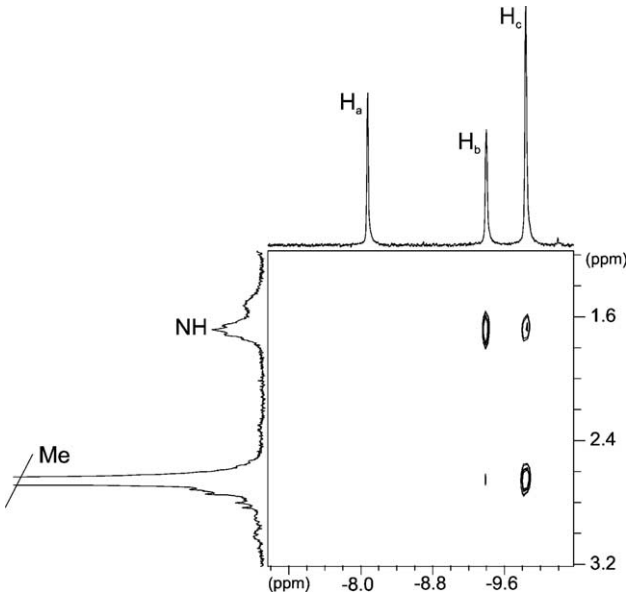

Fig. 4. Selected region of ^{1}H 2D NOESY experiment performed on a CD_2Cl_2 solution of anion **2** (4.7 T, 273 K, τ_m = 0.3 s).

However, the basal hydride H_b has a much stronger cross-peak with the NH signal than with the methyl resonance, the volume ratio between the (NH ⋯ H_b) and (Me ⋯ H_b) cross-peaks being 5.0, in spite of the fact that 6 protons contribute to the latter interaction (see Table 3). On the contrary, the analogous ratio involving the hydrides H_c bridging the lateral edges, was only 0.59.

As reported in Table 3, the distances between the hydrido ligands (as computed by DFT) are virtually insensitive to the conformation of anion **2**. The parameterisation of the nOe volumes with respect to the distances $H_a \cdots H_b$ and $H_a \cdots H_c$ is therefore possible without making any assumption as to the presence in solution of a specific rotamer. The nOe derived distances for the (NH,Me) ⋯ (H_b, H_c) interactions are reported in Table 3, along with the values computed for rotamers A and B employing the DFT optimised geometries and averaging the equivalent interproton vectors assuming a fast rotation of the methyl groups [9]. These values unambiguously confirm the (almost) exclusive presence of rotamer A in dichloromethane solution.

Further experimental evidence of the proton–hydride interaction is usually provided by the shortening of the longitudinal relaxation times T_1 of the hydride, due to the dipolar contribution of the close hydrogen atom [10]. We therefore measured the proton longitudinal relaxation time T_1 of all the hydrides and the NH proton in **2**, in CD_2Cl_2 solution, in the temperature range 175–273 K (see Table 4). Their logarithmic plot versus $1/T$ (shown in Fig. 5) displays the typical "v" shape. The T_1 values measured for H_b and H_c are always shorter than those measured for the hydride H_a, bridging the basal edge in the opposite side of the cluster plane. The values of T_1 for both H_b and H_c reach their minimum value at approximately 193 K. The increase of the relaxation rates of H_b and H_c with respect to H_a (R_{H-H}) is clearly attributable to the dipolar contribution of the NH and methyl protons to the relaxation of these hydrides. From the 2D NOESY experiment it is clear that for the *syn* hydride H_b the main contribution comes from the NH proton. Therefore, estimating (at the minimum of the temperature course of T_1, where the τ_c value is known) the difference between the relaxation rates of the *syn* (H_b) and *anti* (H_a) hydride, it is possible to

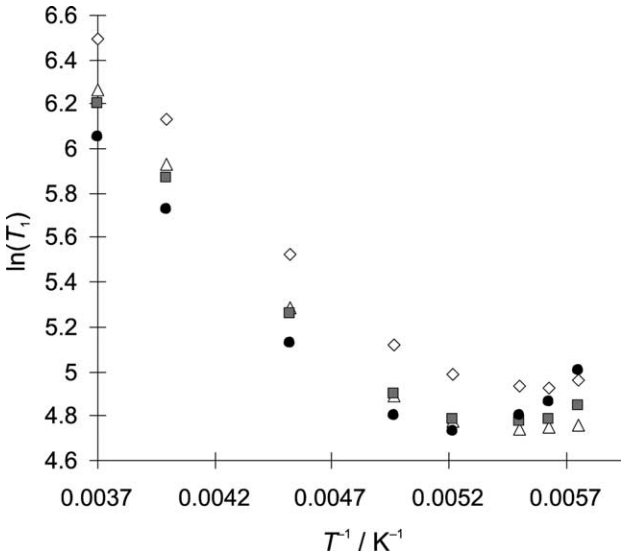

Fig. 5. Temperature dependence of the longitudinal relaxation times of the hydridic and NH resonances in anion **2** (4.7 T, CD_2Cl_2): ◇ H_a, ■ H_b, △ H_c and ● NH.

Table 3
Theoretical (DFT) and experimental (nOe) averaged interproton distances for anion **2**

	$H_a \cdots H_b$	$H_a \cdots H_c$	NH ⋯ H_b	NH ⋯ H_c	Me ⋯ H_b	Me ⋯ H_c
Multiplicity	1	2	1	2	6	12
Averaged DFT distance (rotamer A)	2.448	2.729	2.132	2.563	3.615	2.846
Averaged DFT distance (rotamer B)	2.442	2.755	4.591	3.449	2.967	2.703
Relative nOe volumes (CD_2Cl_2)	0.35	0.30	0.85	0.59	0.17	1.00
Derived distance (CD_2Cl_2)			2.1	2.5	3.7	3.1
Relative nOe volumes (acetone-d_6)	0.35	0.38	0.30	0.27	0.34	1.00
Derived distance (acetone-d_6)			2.5	2.8	3.3	3.1

Table 4
Temperature dependence of T_1 values (ms) for the hydrides and the NH proton of anion **2** in CD_2Cl_2

T [K]	T_1 (H_a)	T_1 (H_b)	T_1(H_c)	T_1(NH)
175	143.4	127.2	116.5	149.5
179	138.1	120.2	115.1	129.1
183	138.7	118.3	114.7	121.4
193	146.3	119.7	118.9	114.0
203	167.3	134.3	133.2	121.4
223	250.1	191.9	197.9	168.4
253	462.7	355.0	375.0	307.3
273	662	493	525	427

calculate the distance r_{H-H} between NH and H_b according to Eq. (1) [11]. The resulting value is 2.24(2) Å [12], in good agreement with the values obtained from the nOe data, the X-ray data and the theoretically derived values,

$$R_{H-H} = (T_1)^{-1}_{H-H} = \frac{\mu_0^2 \gamma_H^4 \hbar^2 I(I+1)}{40\pi^2 r_{H-H}^6} \tau_c \left[\frac{1}{1+\omega_0^2\tau_c^2} + \frac{4}{1+4\omega_0^2\tau_c^2}\right]. \quad (1)$$

In regard to the hydrides bridging the lateral edges (H_c), the 2D NOESY experiment shows that they strongly interact with both the NH and the methyl groups. Therefore, being impossible to separate the contributions of the two different groups of atoms to the relaxation rate of these hydrides, no hydride to ligand distance could be calculated.

^{1}H NMR spectroscopy provide clear evidence of the close approach of the NH proton to the H_b hydride. Short distances between a proton and a hydride are usually taken as proof of the presence of a dihydrogen bond. However, as previously stated, in the present case the dimethylamine conformation might be mainly dictated by the steric hindrance exerted by the diagonal carbonyl ligands, rather then by an attractive proton–hydride interaction.

Evidence that the short NH $\cdots$ (μ-H)Re_2 distance in **2** is not due to steric constraints only but also to the presence of a true dihydrogen bond is provided by IR studies. The presence of a hydrogen bond usually causes a red-shift and a strong broadening of the stretching absorption of the X–H hydrogen bond donor. In this case, the ν(NH) IR band of the coordinated amine of **2** appears at 3262 cm^{-1}, approximately a 100 cm^{-1} shift to lower wavenumbers with respect to the literature value for pure DMA in a solvent not able to act as proton acceptor (3361 cm^{-1} in *n*-hexane) [13]. An hydrogen bonding interaction is therefore shown to be present in **2**, even if it is rather weak. From the IR data it is possible to calculate the enthalpy associated with the hydrogen bond formation, through the empirical Iogansen equation (Eq. (2)) [14]. This correlates the change in position of the stretching band of the X–H bond ($\Delta\nu$) with the hydrogen bond enthalpy. In this case the measured $\Delta\nu$ value corresponds to $\Delta H^\circ = -2.2$ kcal mol^{-1},

$$-\Delta H^\circ = 18\Delta\nu/(\Delta\nu + 720). \quad (2)$$

Further evidence that the proton–hydride interaction significantly contributes to the preferred dimethylamine rotamer present in CH_2Cl_2 is provided by the observation that in a solvent able to act as proton acceptor, different rotamers are present. A 2D NOESY experiment performed at 273 K in acetone-d_6 shows that H_b has a stronger cross-peak with the Me hydrogen atoms than with NH (see Table 3). The nOe derived distances for the (NH,Me) $\cdots$ (H_b,H_c) interactions lie between the average values computed for rotamers A and B. This is in agreement with the presence in acetone-d_6 of a significant amount of both conformers, rotamer B now being stabilized by a conventional hydrogen bond with the oxygen atom of the solvent.

3. Conclusions

The structure of anion **2** has been characterized by NMR spectroscopy, X-ray analysis and DFT computations. The experimental and theoretical data have clearly shown that, both in the solid state and in solution, in the preferred conformation the NH proton of the coordinated amine is directed towards the hydride bridging the opposite cluster edge.

DFT calculations and experimental results indicate that this conformation, beside minimizing steric repulsions between the ligands coordinated to the cluster core, is furthermore stabilized by a weak intra-molecular N–H $\cdots$ (μ-H)Re_2 dihydrogen bond, whose estimated enthalpy is as low as 2.2 kcal mol^{-1}.

In contrast to what is observed for the analogous cluster anion containing an axial pyrazole ligand, anion **2** is very stable at room temperature in dichloromethane solution. Indeed, the weak acidity of the proton donor, reflected by the very low ΔH° value, and the bridging coordination of the proton acceptor, that reduces its thermodynamic and kinetic "hydricity", do not promote the protonation pathway leading to H_2 evolution.

4. Experimental

The reactions were performed under N_2, in solvents dried and deoxygenated by standards methods. Dimethylamine solution (2 M in THF, Aldrich) was used as received. The starting compound [PPh_4][Re_3(μ$_3$-H)(μ-H)$_3$(CO)$_9$] was prepared as described in the literature [15]. The NMR spectra were acquired on Bruker AC200 and DRX300 spectrometers and the IR spectra on a Bruker Vector 22FT instrument.

4.1. Synthesis of [PPh_4][Re_3(μ-H)$_4$(CO)$_9$(DMA)] ([PPh_4]**2**)

A sample (18.6 mg, 0.0161 mmols) of [PPh_4][Re_3(μ$_3$-H)(μ-H)$_3$(CO)$_9$] was dissolved at room temperature in freshly distilled CH_2Cl_2 (5 mL). Addition of dimethylamine (2 M in THF, 10 μL, 0.020 mmols) caused a change in the solution colour. IR (CH_2Cl_2): ν(CO) = 2034 m, 1999vs, 1912vs cm^{-1}. Addition of *n*-hexane gave a yellow precipitate that was dried under vacuum (15.3 mg, 0.0125 mmols, isolated yields 78%). Slow diffusion of *n*-hexane in a CH_2Cl_2 solution of **2** afforded crystals suitable for X-ray analysis. ^{1}H NMR

(CD_2Cl_2, 300 K) $\delta = 2.79$ (d, 6, CH_3, $J_{HH} = 6.3$ Hz), 1.82 (septuplet, 1, NH), −7.92 (s, 1, H_a), −9.26 (s, 1, H_b), −9.70 (s, 2, H_c).

4.2. Variable temperature T_1 and two-dimensional NOESY experiment on **2** in CD_2Cl_2

A solution of [PPh_4]**2** (21.1 mg, 0.0172 mmols) in CD_2Cl_2 (0.5 mL) in an NMR tube was degassed through repeated freeze-thaw cycles. ^{1}H NMR variable temperature spectra were acquired on a 4.7 T instrument from 175 to 273 K, and at each temperature the ^{1}H T_1 values were obtained by a three-parameter fit of the intensities of the signals, in spectra recorded with the standard nonselective inversion recovery pulse sequence, with 14 variable delays. The results are reported in Table 4. The same sample was also used for the ^{1}H two-dimensional NOESY phase-sensitive experiment shown in Fig. 4. It was performed at 273 K, on a 4.7 T field, with $\tau_m = 0.3$ s, 8 FIDs, sweep width = 4347 Hz, 1 K data points for 256 experiments. Shifted sine-bell functions were applied in both dimensions before the Fourier transform and after zero-filling to 1 K in F_1.

4.3. X-ray diffraction structural analysis

Crystal data for [PPh_4]**2**: $[C_{24}H_{20}P]^+[C_{11}H_{11}NO_9Re_3]^- = C_{35}H_{31}NO_9PRe_3$, $M_r = 1199.18$, monoclinic, space group $P2_1/c$ (No. 14), $a = 14.344(4)$, $b = 17.417(4)$, $c = 15.488(4)$ Å, $\beta = 91.18(1)°$, $V = 3868.5(17)$ Å^3, $Z = 4$, $T = 295(2)$ K, graphite-monochromated Mo Kα radiation ($\lambda = 0.71073$ Å), $\rho_{calcd} = 2.059$ g cm^{-3}, $F(000) = 2240$, colourless crystal $0.24 \times 0.18 \times 0.12$ mm^3, μ(Mo Kα) = 9.455 mm^{-1}, empirical absorption correction (SADABS [16], 28470 symmetry equivalent reflections, effective data to parameters ratio: 9.3), minimum/maximum transmission factors 0.166/0.322, Bruker SMART diffractometer, ω scans ($\Delta\omega = 0.3°$), 2400 frames each at 20 s exposure keeping the detector at 5.0 cm from the sample, $1.8 \leqslant \theta \leqslant 25.1°$, index ranges $h = -17 \rightarrow 17$, $k = -20 \rightarrow 20$, $l = -18 \rightarrow 18$, 45369 reflections of which 6854 unique ($R_{int} = 0.0297$, $R_\sigma = 0.0187$), 5865 reflections with $I > 2\sigma(I)$, intensity decay 4%, solution by direct methods (SIR97 [17]) and subsequent Fourier synthesis, anisotropic full-matrix least-squares on F^2 using all reflections (SHELX97 [18]), hydrogen atoms placed in idealised position [19], phenyl groups refined as variable metric regular hexagons, data/parameters 6854/401, $S(F^2) = 1.046$, $R(F, I > 2\sigma(I)) = 0.0424$, $wR(F^2$, all data) = 0.1145, weighting scheme $w = 1/[\sigma^2(F_o^2) + (0.085P)^2 + 26P]$, where $P = (F_o^2 + 2F_c^2)/3$, maximum/minimum residual electron density 2.778/−2.037 e Å^{-3}. CCDC-253668 ([PPh_4]**2**) contains the supplementary crystallographic data for this paper. This data can be obtained free of charge via www.ccdc.cam.ac.uk/conts/retrieving.html or from the Cambridge Crystallographic Data Centre, 12 Union Road, Cambridge CB2 1EZ, UK (fax: (+44)1223-336-033; e-mail: deposit@ccdc.cam.ac.uk).

4.4. Computational study

All the calculations were done using an empirically parameterised density functional theory (DFT) method incorporating Becke's three-parameter hybrid functional along with the Lee–Yang–Parr correlation functional (B3LYP) [20]. A basis set incorporating the "small core" relativistic effective core potentials (ECP) of Hay and Wadt was used for the rhenium atoms along with valence double-ζ functions [21] augmented with an energy-optimised set of 5p functions [22], yielding a final contraction of (341/341/21), similar but different from the basis set LanL2DZ included in GAUSSIAN 03 [23]. The standard valence double-ζ basis set with a single polarization function 6-31G(d,p) [24] was used for all remaining atoms. Geometries were optimised in redundant internal coordinates [25], employing the GDIIS algorithm [26], until the maximum (root-mean-square) force was less than 0.00045 (0.00030) a.u. The energy profile shown in Fig. 3 was computed freezing the (improper) torsion angle ω to the values from 20° to 160° in steps of 20° and allowing all the remaining internal coordinates to relax. Calculations were done without the imposition of any symmetry except for the two proposed minima (rotamer A and B) which were found to possess C_s symmetry. Analytic frequency computations were done for the two proposed minima (rotamer A and B), for free dimethylamine and for the dimethylamine dimer. A complete list of coordinates and frequencies can be requested of the authors (P.M.). All the computations were performed with GAUSSIAN 03 [23].

References

[1] J.C. Lee, A.L. Rheingold, B. Muler, P.S. Pregosin, R.H. Crabtree, Chem. Commun. (1994) 1021.
[2] L.M. Epstein, E.S. Shubina, Coord. Chem. Rev. 231 (2002) 165.
[3] (a) S. Aime, R. Gobetto, E. Valls, Organometallics 16 (1997) 5140;
(b) S. Aime, M. Férriz, R. Gobetto, Organometallics 18 (1999) 2030;
(c) S. Aime, E. Diana, R. Gobetto, M. Milanesio, E. Valls, D. Viterbo, Organometallics 21 (2002) 50.
[4] T. Beringhelli, G. D'Alfonso, M. Panigati, P. Mercandelli, A. Sironi, Chem. Eur. J. 8 (2002) 5340.
[5] (a) T. Beringhelli, G. D'Alfonso, Chem. Commun. (1994) 2631;
(b) T. Beringhelli, G. D'Alfonso, M. Panigati, F. Porta, P. Mercandelli, M. Moret, A. Sironi, Organometallics 17 (1998) 3282.
[6] (a) T. Beringhelli, G. Ciani, G. D'Alfonso, H. Molinari, A. Sironi, Inorg. Chem. 24 (1985) 2666;
(b) G. Ciani, G. D'Alfonso, M. Freni, P. Romiti, A. Sironi, A. Albinati, J. Organomet. Chem. 136 (1977) C49;

(c) T. Beringhelli, G. D'Alfonso, M. Freni, G. Ciani, A. Sironi, Dalton Trans. (1986) 2691.
[7] The hydrido ligand was placed in a potential energy optimised position using the program HYDEX: A.G. Orpen, Dalton Trans. (1980) 2509. The N–H bond distance was fixed to the average value found for aliphatic amine by neutron diffraction (1.025 Å): CSD (version 5.24, November 2002). F.H. Allen, Acta Crystallogr., Sect. B: Struct. Sci. 58 (2002) 380.
[8] The averaged distance has been computed as $\langle d \rangle = \int d(q) e^{-E(q)/RT} dq / \int e^{-E(q)/RT} dq$ in which $E(q) = 1/2kq^2$.
[9] To average the equivalent interproton distances the Tropp's equation has been employed. D. Neuhaus, M.P. Williamson, The Nuclear Overhauser Effect in Structural and Conformational Analysis, second ed., Wiley-VCH, New York, 2000, pp. 167–178.
[10] S. Aime, E. Diana, R. Gobetto, M. Milanesio, E. Valls, D. Viterbo, Organometallics 21 (2002) 50, and refs therein.
[11] A. Abragam, The Principles of Nuclear Magnetism, Oxford University Press, Oxford, UK, 1973 (Chapter 8).
[12] The standard deviation on the computed distance were obtained by propagation of errors starting from the T_1 values 146.3(10) and 119.7(4) ms for H_a and H_b at 193 K.
[13] H. Wolff, G. Gamer, J. Phys. Chem. 76 (1972) 871.
[14] A.V. Iogansen, Hydrogen Bond, Nauka, Moscow, 1981, cited in; N.V. Belkova, E.S. Shubina, A.V. Ionidis, L.M. Epstein, H. Jacobsen, A. Messmer, H. Berke, Inorg. Chem. 36 (1997) 1522.
[15] T. Beringhelli, G. D'Alfonso, M.G. Garavaglia, Dalton Trans. (1996) 1771.
[16] G.M. Sheldrick, SADABS, Universität Göttingen, Germany, 1996.
[17] A. Altomare, M.C. Burla, M. Camalli, G.L. Cascarano, C. Giacovazzo, A. Guagliardi, A.G.G. Moliterni, G. Polidori, R. Spagna, J. Appl. Crystallogr. 32 (1999) 115.
[18] G.M. Sheldrick, SHELX97, Universität Göttingen, Germany, 1997.
[19] A.G. Orpen, Dalton Trans. (1980) 2509.
[20] (a) A.D.J. Becke, Chem. Phys. 98 (1993) 5648;
(b) C. Lee, W. Yang, R.G. Parr, Phys. Rev. B 37 (1988) 785.
[21] P.J. Hay, W.R.J. Wadt, Chem. Phys. 82 (1985) 299.
[22] M. Couty, M.B. Hall, J. Comput. Chem. 17 (1996) 1359.
[23] GAUSSIAN 03 (Revision B.04), Gaussian Inc., Pittsburgh, PA, 2003.
[24] W.J. Hehre, L. Radom, P.v.R. Schleyer, J.A. Pople, Ab Initio Molecular Orbital Theory, Wiley, New York, 1986.
[25] C. Peng, P.Y. Ayala, H.B. Schlegel, M.J. Frisch, J. Comput. Chem. 17 (1996) 49.
[26] P. Császár, P. Pulay, J. Mol. Struct. 114 (1984) 31.